ELSEVIER

Chemical Engineering Journal 137 (2008) 603–613

Chemical Engineering Journal

www.elsevier.com/locate/cej

Simulation and optimization of silicon thermal CVD through CFD integrating Taguchi method

W.T. Cheng *, H.C. Li, C.N. Huang

Department of Chemical Engineering, National Chung Hsing University, Taichung 402, Taiwan, ROC

Received 25 November 2006; received in revised form 12 May 2007; accepted 16 May 2007

Abstract

A steady laminar flow coupled with heat transfer, gas-phase chemistry, and surface chemistry model, was numerically solved for optimization of thermal chemical vapor deposition (CVD) from a gas mixture of silane and helium in the axis-symmetrical rotating/stagnating reactor with and without a rotational showerhead. At first, through computational fluid dynamics (CFD), the rate of deposited silicon on substrate was calculated and validated with the benchmark solutions from the literature. The computational model was then integrated with the dynamic model of Taguchi method to optimize the process parameters formulating a correlation to minimize thickness deviation of deposited silicon film on the substrate in the different sizes. In particular, the result shows thickness deviation of deposited silicon film can be reduced to 5.8% and 11% from 18% and 36% over a wafer in the diameters of 0.15 m and 0.3 m, respectively, in the thermal CVD process with the optimal conditions in this work.

Keywords: Simulation; Optimization; CFD; Thermal CVD; Silicon; Taguchi method

1. Introduction

In manufacturing semi-conductor [1,2] and thin film transistor liquid crystal display (TFTLCD) [3], chemical vapor deposition (CVD) constitutes an important technology to fabricate silicon film that can be oxidized by thermal process producing silicon dioxide for gate or capacitor dielectric, insulator, primary passive layer, mask against diffusion or etching process, and so on.

To describe hydrodynamics and transport phenomena, Wahl [4] introduced the computational era in CVD reactor model. Later, Coltrin et al. [5] formulated the CVD gas-phase chemistry with elementary reactions replacing lumped chemistry. Based on this model, Tirtowidjojo and Pollard [6] developed the surface chemistry in CVD.

In short, the developed models of CVD may be roughly divided into two categories: (a) reactor model for simulation of multi-dimensional flow and transport phenomena in relation to process operation and equipment design problems in the presence of the simple CVD chemistry [7–11] and (b) chemistry model for the unraveling of detailed reaction mechanisms in the gas-phase and at the surface in zero or one-dimensional hydrodynamic reactor [5,12–16].

It is worth mentioned that Kleijn [17] studied two-dimensional computation fluid dynamics (CFD) for the full multi-component transport phenomena, the multi-species, and multi-reaction chemistry in thermal CVD with rotational disk/stagnation flow to produce silicon film, which results was validated against the well-known one-dimensional SPIN code from SANDIA by Kee et al. [18] and Coltrin et al. [19,20] and might be used as the benchmark solutions for the simulations of thermal CVD.

As for the optimization of system, Taguchi method is a scientific and disciplined mechanism for evaluating and implementing improvements in products, processes, materials, equipment, and facilities [21]. Particularly, Taguchi method can be used to adopt the fundamental ideal to simplify and standardize the factorial and fractional designs leading to the experiments more consistent with the results.

Rajkumar et al. [22] employed Taguchi method to optimize process parameters involving the squeegee pressure, squeegee speed, stencil-substance separation speed and squeegee print direction, for flip chip stencil printing. The computer simulation with Taguchi's route has been proposed to solve the problems of integrated manufacturing system [23]. Furthermore, by using Taguchi method, Wang et al. [24] optimized the operational

* Corresponding author. Tel.: +886 4 22857325; fax: +886 4 22854734.
E-mail address: wtcheng@dragon.nchu.edu.tw (W.T. Cheng).

1385-8947/$ – see front matter © 2007 Published by Elsevier B.V.
doi:10.1016/j.cej.2007.05.042

Nomenclature

A	variable of the orientation of rotational showerhead
A_k	homogenous reaction rate with respect to kth gas-phase (mol m^3/s)
B	variable of the inlet silane mole fraction
C	variable of the flow rate of reactant (mol/s)
C_p	specific heat at constant pressure (J/(mol K))
D	variable of the temperature of reactant (K)
D_i^{eff}	the effective diffusion coefficient with respect to i species (m^2/s)
E	variable of showerhead rotation rate (rad/s)
E_k	activation energy of kth gas-phase reaction (J/mol)
f_i	mole fraction of ith gas species
F	variable of the temperature of the substrate (K)
G	variable of susceptor rotational rate (rad/s)
dh/dt	the growth rate of silicon film (m/s)
H	variable of the operational pressure (atm)
H_i^0	the standard heat of formation of ith gas species (J/mol)
ΔH_k^0	the difference of the standard heat of formation of kth gas species (J/mol)
I	the unit tensor
$\vec{j}_i$	mass flux of ith gas species (kg/(m^{2}s))
$k_{k,b}^g$	the rate constant of reverse reaction for kth gas species (mol m^3/s)
$k_{k,eq}^g$	the equilibrium constant of homogeneous kth gas reaction
$k_{k,f}^g$	the constant of forward reaction for kth gas species (mol m^3/s)
L	orthogonal array
M	the different diameters of wafer defined as $M1$, $M2$, and $M3$, respectively (m)
M_i	the molar mass of ith species (kg/mol)
M_{si}	the molecular weight of silicon (kg/mol)
n	the effective divisor defined in Eq. (18)
N	species number
P	the pressure in the reactor (atm)
r	radial coordinate (m)
R	the gas constant, 8.34132 (J/(mol K))
R_s	radius of the susceptor (m)
R^s	the molar flux for the decomposition of gas-phase species at the surface (mol/(m^2 s))
R_k^g	gas-phase reaction rate (mol/(m^3 s))
R_{max}^s	the maximum rate of deposition silicon on the substrate (mol/(m^2 s))
R_{min}^s	the minimum of deposition rate silicon on substrate (mol/(m^2 s))
S	the sensitivity defined in Eq. (16)
S_β	regressive deviation defined in Eq. (19)
S_i^0	the standard entropy of ith gas species (J/(mol K))
ΔS_k^0	the difference of the standard entropy of kth gas species (J/(mol K))
S_T	the total square amount of film thickness deviation defined in Eq. (21) (m)
T	temperature in the reactor (K)
T_s	the temperature on the substrate (K)
u	velocity (m/s)
U_{in}	a uniform velocity from the showerhead (m/s)
V_e	deviation of error defined in Eq. (20)
w_i	gas species i mass fraction
y	the ideal function of film thickness deviation defined in Eq. (14)
z	axial coordinate (m)

Greek symbols

Ω_1	angular velocity of showerhead (rad/s)
Ω_2	angular velocity of susceptor (rad/s)
β	the linearity defined in Eq. (17)
γ_i	the reactive sticking coefficient of species i
η	the ratio of signal to noise defined in Eq. (15)
λ	thermal conductivity of gas mixture (W/(m K))
μ	viscosity of gas mixture (kg/(m s))
ν_{ik}	net stoichiometry coefficients of gas-phase
ν_{ik}^b	stoichiometry coefficients of backward gas reaction
ν_{ik}^f	stoichiometry coefficients of forward gas reaction
ρ	density of gas mixture (kg/m^3)
ρ_{si}	the density of silicon (kg/m^3)
τ	shear stress (kg m/s^2)

conditions of simultaneous supercritical fluid extraction and chemical derivation for the gas chromatographic–mass spectrometric determination of amphetamine and methamphetamine in an aqueous matrix.

In addition, Taguchi method was employed to analyze influences of the moisture absorption on plastic ball grid array (PBGA) of package's warp during IR re-flow process [25]. The effects of the selected process parameters on the casting density and the subsequent optimal settings of the parameters have been accomplished with Taguchi method [26].

In this work, a steady laminar thermal flow associated with multi-species and multi-chemical reactions in the axis-symmetrical rotating and stagnating reactor with and without a rotational showerhead is solved by the CFD technique to re-examine the growth of silicon film on the wafer during thermal CVD process. After validating the obtained numerical results with the benchmark solutions [17], the dynamic model of Taguchi method is applied to optimize the process conditions involving angular velocity of showerhead and susceptor, the rotational orientation of showerhead to susceptor, the temperature of reactor, concentration of reactants, operational pressure, and the temperature of susceptor to reduce thickness deviation of deposited silicon film on the substrate in the different sizes.

To sum up, this research intents to formulate a correlation through integration of CFD with Taguchi method to predict thickness deviation of deposited silicon film varying with the

size of substrate in thermal CVD process for practice applications.

2. Problem formulation

2.1. Physical model

In this investigation, the steady and two-dimensional laminar flow coupled with heat-transfer, and gas-phase chemistry as well as surface chemistry in the axis-symmetrical rotating and stagnating reactor quipped with rotational showerhead, is considered to simulate forming silicon film in a thermal CVD reactor, as shown in Fig. 1, by mans of CFD. According to the system proposed by Kleijn [17], the studied physical model may be described below.

A gas mixture, which the mole fraction of silane is 0.001 and the rest is helium, is charged into the reactor at temperature $T_{in} = 300$ K and velocity U_{in} from the showerhead with and without an angular velocity Ω_1. A susceptor in diameter of $2R_s = 0.3$ m and with temperature, $T_s = 1000$ K, is placed a distance of 0.1 m below the inlet. The reactions of gas–solid are carried out to produce silicon film on wafer placed on the susceptor that rotates around its axis with and without an angular velocity Ω_2 at atmosphere. Furthermore, the inner and the outer wall of the reactor are adiabatic and static, respectively.

Two cases are considered: (1) one is set as $\Omega_1 = \Omega_2 = 0$ and $U_{in} = 0.10$ m/s, which the velocity, temperature, and concentrations are strongly non-uniform in radius, to validate the present work against the benchmark solution [17]; (2) another, which process parameters and their levels are listed in Table 1, is used to optimize the thermal CVD process by CFD integrating with the Taguchi method for the uniformity of deposited silicon film over the substrate in the different sizes.

2.2. Mathematical model

The gas mixture is treated as a continuum and an incompressible ideal gas in reactor. The low Mach number is assumed for the laminar flow. Effects of buoyancy and heat radiation are neglected. The composition of the N-component gas mixture is described by the dimensionless mass fractions w_i ($i = 1, 2, 3, \ldots, N$) of species, which sums up to unity. The diffusion of gas

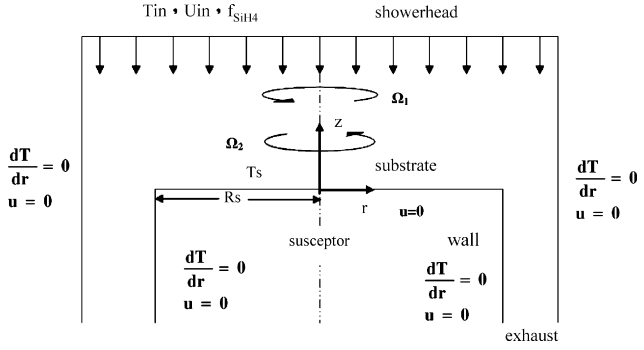

Fig. 1. The system and boundary conditions for thermal silicon CVD process in this study.

Table 1
Controlled factors and levels assignments for optimization of silicon thermal CVD process through CFD integrated with Taguchi method in this investigation

Factors	Levels		
	1	2	3
(A) Rotational orientation of showerhead to suscepctor	Parallel	Opposite	
(B) Mole fraction of SiH4	0.001[a]	0.003	0.005
(C) Inlet flow rate (m/s)	0.05	0.1[a]	0.2
(D) Inlet flow temperature (K)	300[a]	400	500
(E) Angular velocity of showerhead (rad/s)	0[a]	30	60
(F) Susceptor's temperature (K)	800	1000[a]	1200
(G) Angular velocity of substrate (rad/s)	0[a]	300	600
(H) Operational pressure (atm)	0.9	0.95	1[a]

[a] From Kleijn [17].

species is expressed by the mass fluxes $\vec{j}_i$ with respect to the mass averaged velocity u, which sums up to zero. The heats of inter-diffusion of species and chemical reaction are not considered. Furthermore, the pressure diffusion, forced diffusion, and thermal diffusion are negligible.

According to the above assumptions, the transports of momentum, heat and mass can be mathematically described by the continuity equation, the Navier–Stokes equation, and energy equation as well as mass conservation of the ith gas species under steady state as follows [27]:

(1) Continuity equation

$$\nabla \cdot (\rho u) = 0 \tag{1}$$

here $\rho = PM_{He}/RT$ is the density of the helium which is equal to that of the gas mixture in reactor [28], where P is the pressure in reactor, R the gas constant, and T is temperature in the gas stream.

(2) Equation of motion

$$\nabla \cdot \rho u u + \nabla P + \nabla \cdot \tau = 0 \tag{2}$$

where u is velocity vector and τ is shear stress expressed by

$$\tau = \mu(\nabla u + (\nabla u)^{\mathrm{T}}) - \left(\frac{2}{3}\mu\right)(\nabla \cdot u)I \tag{3}$$

for the Newtonian fluid. In Eq. (3), $\mu = 5.09 \times 10^{-7} T^{0.64}$ (kg m^{-1} s^{-1}) is the viscosity of gas mixture [28] and I indicates the unit tensor.

(3) Energy equation

$$C_p \nabla \cdot (\rho u T) - \nabla \cdot (\lambda \nabla T) = 0 \tag{4}$$

where $C_p = 5193$ (J mol^{-1} K^{-1}) is specific heat of the gas mixture and $\lambda = 3.96 \times 10^{-3} T^{0.64}$ (W m^{-1} s^{-1}) is heat conductivity [28].

(4) Species conservation equations

$$-\nabla \cdot (\rho u w_i) - \nabla \cdot j_i + M_i \sum_{k=1}^{k} \nu_{ik} R_k^{g} = 0 \tag{5}$$

where $\vec{j}_i$ is the mass flux of ith species, defined by

$$j_i = -\rho D_i^{\text{eff}} \nabla w_i \tag{6}$$

in which D_i^{eff} is the effective diffusion coefficient [27], M_i and ν_{ik} the molar mass of ith component and net stoichiometric coefficients defined as $\nu_{ik} = \nu_{ik}^{\text{b}} - \nu_{ik}^{\text{f}}$ and R_k^{g} is net molar reaction rates expressed by

$$R_k^{\text{g}} = k_{k,f}^{\text{g}} \prod_{\text{reactant}} \left(\frac{Pf_i}{RT}\right)^{\nu_{ik}^{\text{f}}} - k_{k,b}^{\text{g}} \prod_{\text{products}} \left(\frac{Pf_i}{RT}\right)^{\nu_{ik}^{\text{b}}}. \tag{7}$$

In Eq. (7), the rate constant of forward reaction is a function of temperature as

$$k_{k,\text{f}}^{\text{g}}(T) = A_k T^{\beta_k} \exp\left(\frac{-E_k}{RT}\right) \tag{8}$$

where values of A_k, β_k and E_k were listed in literature [15]; and the rate constants of kth reversible gas-phase, $k_{k,\text{b}}^{\text{g}}$, can be calculated from the rate constants of forward reaction and the thermo-chemistry [5], namely,

$$k_{k,\text{b}}^{\text{g}} = \frac{k_{k,\text{f}}^{\text{g}}}{k_{k,\text{eq}}^{\text{g}}} \tag{9}$$

where the equilibrium constant of homogenous reaction is given by

$$k_{k,\text{eq}}^{\text{g}} = \exp\left(\frac{T\,\Delta S_k^0 - \Delta H_k^0}{RT}\right)\left(\frac{P}{RT}\right)^{\sum_{k=1}^{N}\nu_{ik}} \tag{10}$$

where

$$\Delta H_k^0(T) = \sum_{i=1}^{N} \nu_{ik} H_i^0(T); \qquad \Delta S_k^0 = \sum_{i=1}^{N} \nu_{ik} S_i^0(T) \tag{11}$$

which, H_i^0 and S_i^0 are the standard heat of formation and standard entropy, respectively, for ith species [17], as shown in Table 2. In addition, f_i is the mole fractions of the ith species and P is the pressure in reactor. The 26 reversible reactions in gas-phase are listed in Table 3.

3. Computational fluid dynamics

A commercial code, FLUENT version 5.2, containing the SIMPLE algorithm and the QUICK second order interpolation scheme, is used to simultaneously solve equations of continuity (1), motion (2), heat and mass (3 and 4) subject to boundary conditions described in Fig. 1 for velocity field, temperature profile, and the concentration distribution in thermal silicon CVD process. The computational grid is validated by varying number of grid points between 50 and 100 in radial direction as well as between 70 and 150 in the axial direction. These computational grids are tuned until the deviation of deposited rate is less than 0.1%. Afterwards, the molar reaction rate, R^{s}, for the decomposition rate of gas species i on the substrate is obtained by

$$R^{\text{s}} = \frac{\gamma_i}{1-(\gamma_i/2)} \frac{Pf_i}{(2\pi M_i RT_{\text{s}})^{1/2}} \tag{12}$$

where γ_i is the reactive sticking coefficient of species i ($0 \le \gamma_i \le 1$) [20], as listed in Table 4, in where the sticking coefficient of Si_3H_8 is 0; the sticking coefficient of

Table 2
The standard heat of formation, standard entropy, and standard heat capacity in the gas mixture [17]

Species	H_{298}^0 (kcal/mol)	S_{298}^0 (J/mol per K)	$C_{\text{P},298}$ (J/mol per K)
H	218.00	114.6	20.29
H_2	0.00	130.6	28.85
He	0.00	126.0	20.79
Si	450.62	167.9	22.3
SiH	383.68	184.9	29.17
SiH_2	269.05	207.1	34.75
SiH_3	200.00	216.4	40.17
SiH_4	34.31	204.2	43.18
Si_2	589.95	229.9	33.99
Si_2H_2	374.50	246.2	44.49
Si_2H_3	442.25	276.5	64.16
H_2SiSiH_2	263.98	279.9	71.92
H_3SiSiH	312.33	290.3	68.05
Si_2H_5	233.05	291.5	75.78
Si_2H_6	79.92	273.7	79.94
Si_3	635.98	267.8	55.13
Si_3H_8	120.92	348.3	117.91

Table 3
Gas-phase reaction and forward rate constants in Eq. (8) [15]

k	Reactions	A_k	β_k	E_k (kJ/mol)
1	$SiH_4 \Leftrightarrow SiH_2 + H_2$	1.09×10^{25}	−3.37	256
2	$SiH_4 \Leftrightarrow SiH_3 + H$	3.69×10^{15}	0.0	390
3	$Si_2H_6 \Leftrightarrow SiH_4 + SiH_2$	3.24×10^{29}	−4.24	243
4	$SiH_4 + H \Leftrightarrow SiH_3 + H_2$	1.46×10^{7}	0.0	10
5	$SiH_4 + SiH_3 \Leftrightarrow Si_2H_5 + H_2$	1.77×10^{6}	0.0	18
6	$SiH_4 + SiH \Leftrightarrow Si_2H_3 + H_2$	1.45×10^{6}	0.0	8
7	$SiH_4 + SiH \Leftrightarrow Si_2H_5$	1.43×10^{7}	0.0	8
8	$SiH_2 \Leftrightarrow Si + H_2$	1.06×10^{14}	−0.88	189
9	$SiH_2 + H \Leftrightarrow SiH + H_2$	1.39×10^{7}	0.0	8
10	$SiH_2 + H \Leftrightarrow SiH_3$	3.81×10^{7}	0.0	8
11	$SiH_2 + SiH_3 \Leftrightarrow Si_2H_5$	6.58×10^{6}	0.0	8
12	$SiH_2 + Si_2 \Leftrightarrow Si_3 + H_2$	3.55×10^{5}	0.0	8
13	$SiH_2 + Si_3 \Leftrightarrow Si_2H_2 + Si_2$	1.43×10^{5}	0.0	68
14	$H_2SiSiH_2 \Leftrightarrow Si_2H_2 + H_2$	3.16×10^{14}	0.0	222
15	$Si_2H_6 \Leftrightarrow H_3SiSiH + H_2$	7.94×10^{15}	0.0	236
16	$H_2 + SiH \Leftrightarrow SiH_3$	3.45×10^{7}	0.0	8
17	$H_2 + Si_2 \Leftrightarrow Si_2H_2$	1.54×10^{7}	0.0	8
18	$H_2 + Si_2 \Leftrightarrow SiH + SiH$	1.54×10^{7}	0.0	168
19	$H_2 + Si_3 \Leftrightarrow Si + Si_2H_2$	9.79×10^{6}	0.0	198
20	$Si_2H_5 + H_2 \Leftrightarrow Si_2H_3 + H_2$	3.16×10^{14}	0.0	222
21	$Si_2H_2 + H \Leftrightarrow Si_2H_3$	8.63×10^{8}	0.0	8
22	$H + Si_2 \Leftrightarrow SiH + Si$	5.15×10^{7}	0.0	22
23	$SiH_4 + H_3SiSiH \Leftrightarrow Si_3H_5$	6.02×10^{7}	0.0	0
24	$SiH_2 + Si_2H_6 \Leftrightarrow Si_3H_5$	1.81×10^{8}	0.0	0
25	$SiH_3 + Si_2H_5 \Leftrightarrow Si_3H_8$	3.31×10^{7}	0.0	0
26	$H_3SiSiH \Leftrightarrow H_2SiSiH_2$	1.15×10^{20}	−3.06	28

Table 4
Reactive sticking coefficient of Eq. (12) [20]

Species i	γ_i (reactive sticking coefficient)
SiH	1.0
SiH_2	1.0
SiH_3	1.0
SiH_4	$0.0537\exp(-9400/T_s)$
Si_2H_2	1.0
Si_2H_3	1.0
H_2SiSiH_2	1.0
H_3SiSiH	1.0
Si_2H_5	1.0
Si_2H_6	$0.537\exp(-9400/T_s)$
Si_3H_8	0.0

Si_2H_5 is 1; and for others, the values were expressed by

$$\gamma_{Si_2H_6} = 10\gamma_{SiH_4} = 0.537\exp\left(\frac{-9400}{T_s}\right) \quad (13)$$

and $\gamma_i = 1$ for all remaining silicon containing species [15]. Furthermore, in Eqs. (12) and (13) T_s is the temperature of susceptor.

4. Taguchi method

If the process has an input signal that can be directly used to decide the output signal, the optimization will involve determining the best levels of control factor so that the ratio of input signal/output signal is closest to the desired relationship. This is called the dynamic model of Taguchi method [21]. The aim of the Taguchi method is employed to minimize variations of output signal and reduce noise through linearity relationship of the input and output signals in process.

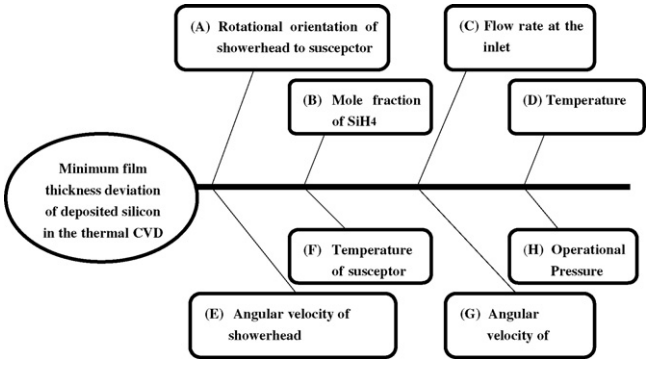

Fig. 2. Selected factors for optimization of thermal CVD process minimizing the thickness deviation of deposited silicon film on wafer in the different sizes.

In this work, the slope of dynamic model of Taguchi method is used to optimize the thermal CVD process for the uniformity of silicon film on the wafer in the different sizes. The objective function of the thickness deviation of deposited silicon film (y) varying with the sizes of wafer (M) is defined by

$$y\,(\%) = \frac{R^s_{max} - R^s_{min}}{R^s_{max}} \times 100 = \beta M \quad (14)$$

where R^s_{max} and R^s_{min} are the maximum and minimum deposition rates of silicon calculated from Eq. (12), respectively, and β is a slope, which is smaller-the-better, dominating by the process parameters, as shown in Fig. 2. Table 5 shows 18 orthogonal array for simulating the effect of these eight factors on the film thickness deviation of deposited silicon on the substrate in the different sizes in the thermal CVD process. Where A is assigned as the orientation of the rotational showerhead to susceptor; B is assigned as the mole fraction of silane at inlet; C is assigned as the flow rate of the reactant; D is assigned as the temperature of the reactant; E is assigned as the angular velocity of the showerhead; F is assigned as the temperature of the substrate;L G is

Table 5
$L18$ orthogonal arrays for 1 factor with 2 level and 7 factors with 3 levels of simulating silicon thermal CVD process

Simulation no.	Factors and its levels								Input signal and its levels (M)[a]		
	(A)	(B)	(C)	(D)	(E)	(F)	(G)	(H)			
$L1$	1	1	1	1	1	1	1	1	$M1$	$M2$	$M3$
$L2$	1	1	2	2	2	2	2	2	$M1$	$M2$	$M3$
$L3$	1	1	3	3	3	3	3	3	$M1$	$M2$	$M3$
$L4$	1	2	1	1	2	2	3	3	$M1$	$M2$	$M3$
$L5$	1	2	2	2	3	3	1	1	$M1$	$M2$	$M3$
$L6$	1	2	3	3	1	1	2	2	$M1$	$M2$	$M3$
$L7$	1	3	1	2	1	3	2	3	$M1$	$M2$	$M3$
$L8$	1	3	2	3	2	1	3	1	$M1$	$M2$	$M3$
$L9$	1	3	3	1	2	2	1	2	$M1$	$M2$	$M3$
$L10$	2	1	1	3	3	2	2	1	$M1$	$M2$	$M3$
$L11$	2	1	2	1	3	3	3	2	$M1$	$M2$	$M3$
$L12$	2	1	3	2	1	1	1	3	$M1$	$M2$	$M3$
$L13$	2	2	1	2	2	1	3	2	$M1$	$M2$	$M3$
$L14$	2	2	2	3	3	2	1	3	$M1$	$M2$	$M3$
$L15$	2	2	3	1	1	3	2	1	$M1$	$M2$	$M3$
$L16$	2	3	1	3	2	3	1	2	$M1$	$M2$	$M3$
$L17$	2	3	2	1	3	1	2	3	$M1$	$M2$	$M3$
$L18$	2	3	3	2	1	2	3	1	$M1$	$M2$	$M3$

[a] Three diameters of substrate studied in this work.

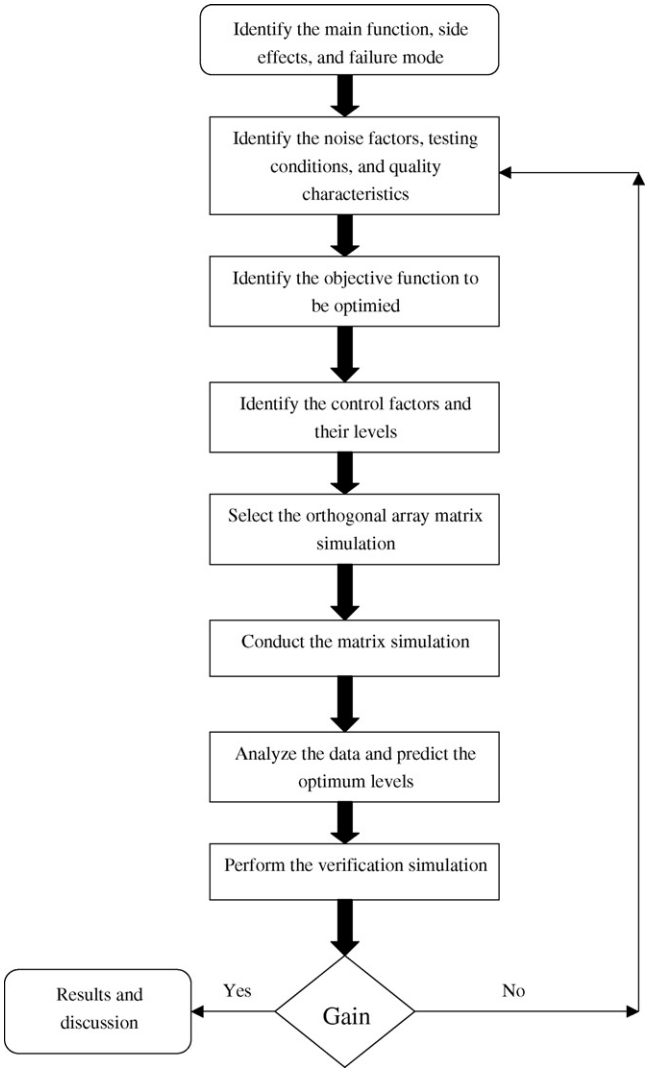

Fig. 3. Flow chart of optimum process with Taguchi method.

assigned as the angular velocity of the susceptor; H is assigned as the operational pressure. Furthermore, one, two, and three represent the level of the factor. For example, for simulation number 1, every factor is assigned as level one; and for simulation number 5, some factors are assigned as level 1 and some factors are assigned as level 2 or 3. In addition, the diameters of the wafer are selected as 0.15 m, 0.2 m, and 0.3 m, expressing by $M1$, $M2$, and $M3$, respectively, in this study.

Fig. 3 displays the flowchart to optimize the thermal CVD process forming silicon film. In where, the ratio of input signal to noise signal abbreviated as SN ratio (η), the sensitivity (S), and the slope (β) can be respectively calculated by [21]

$$\eta = 10\log\left[\frac{(1/n)(S_\beta - V_e)}{V_e}\right]; \quad (15)$$

$$S = 10\log\left[\frac{1}{n}(S_\beta - V_e)\right] \quad (16)$$

$$\beta = \frac{1}{n}(M1y_1 + M2y_2 + M3y_3) \quad (17)$$

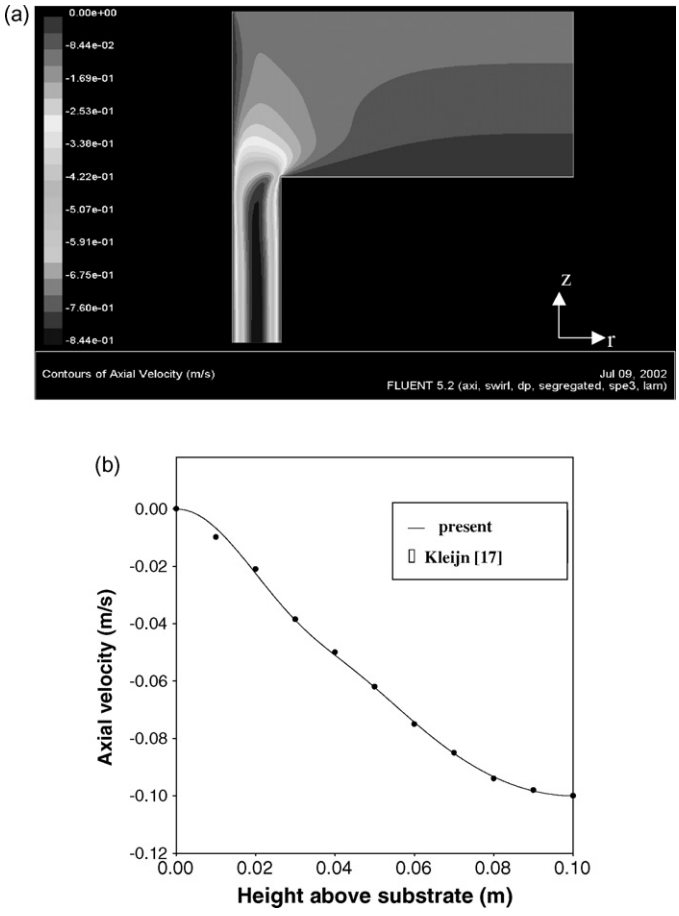

Fig. 4. (a) Velocity contour and (b) velocity profiles at axial direction as a function of the height above the susceptor, for $\Omega_1 = \Omega_2 = 0$, at $r = 0$, where continuous lines are computed in the present and solid circles from Kleijn [17].

As defined in Eq. (16), the sensitivity might be used to regulate the operational conditions to meet the object when the SN ratio (η) is too small [21]. Additionally, in Eqs. (15)–(17), the effective divisor,

$$n = M1^2 + M2^2 + M3^2; \quad (18)$$

Table 6
Comparison of the presented optimum conditions with the process parameters from Kleijn [17] for silicon thermal CVD process

Factor	Kleijn [17]	Optimum
(A) Rotational orientation of showerhead to suscepctor	[a]	Opposite
(B) Mole fraction of SiH4	0.001	0.001
(C) Inlet flow rate (m/s)	0.1	0.1
(D) Inlet flow temperature (K)	300	400
(E) Angular velocity of showerhead (rad/s)	0	30
(F) Susceptor temperature (K)	1000	1200
(G) Angular velocity of substrate (rad/s)	0	300
(H) Operational Pressure (atm)	1	0.95

[a] Static showerhead.

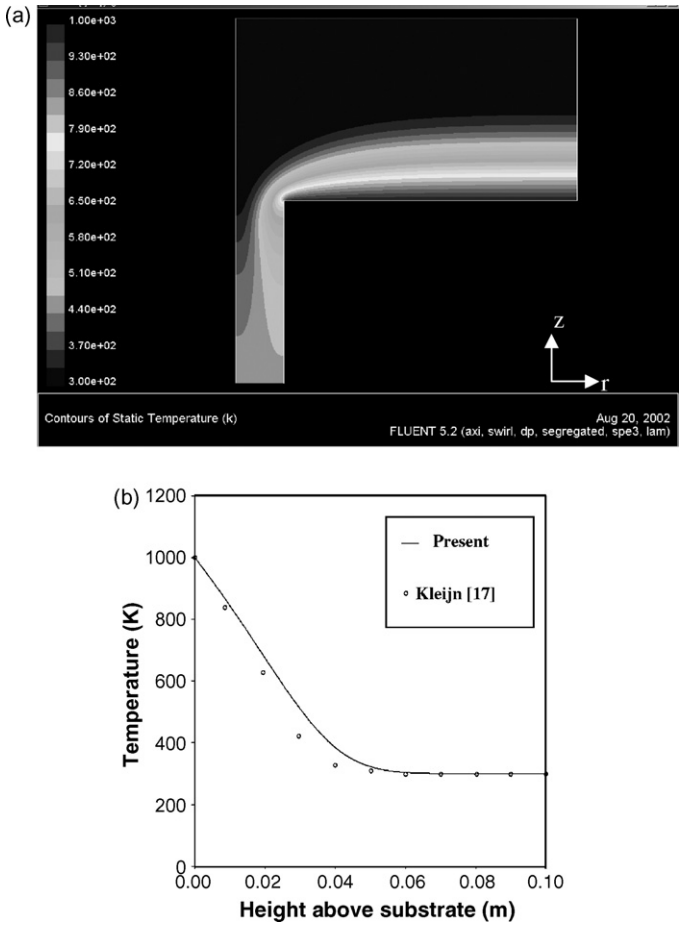

Fig. 5. (a) Temperature contour and (b) temperature profiles at axial direction as a function of the height above the susceptor, at $T_s = 1000$ K and $\Omega_1 = \Omega_2 = 0$, at $r = 0$, where continuous lines are computed in the present and solid circles obtained from Kleijn [17].

the regressive deviation,

$$S_\beta = \frac{(M1y_1 + M2y_2 + M3y_3)^2}{n}; \tag{19}$$

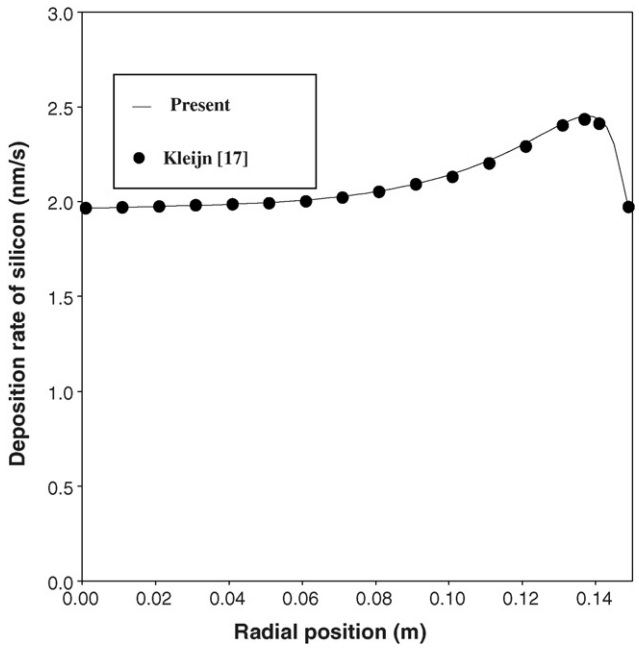

Fig. 6. Radial total deposition rate, at $T_s = 1000$ K and $\Omega_1 = \Omega_2 = 0$, where continuous lines are computed in the present and solid circles obtained from Kleijn [17].

and the error variance,

$$V_e = \frac{S_T - S_\beta}{2} \tag{20}$$

where, S_T, the sum square of film thickness difference of deposited silicon varying with the sizes of wafer (i.e., $M1 = 0.15$, $M2 = 0.2$, and $M3 = 0.3$ m) is obtained by

$$S_T = y_1^2 + y_2^2 + y_3^2. \tag{21}$$

Table 7
Comparison of the present with literatures [17,19] of deposited silicon rate on the substrate for the various gas species at the center of substrate ($r = 0$) at $\Omega_1 = \Omega_2 = 0$, and $T_s = 1000$ K

Species	Deposition rate (nm/s) from Coltrin [19]	Deposition rate (nm/s) from Kleijn [17]	Present (nm/s)
SiH	1.99×10^{-4}	2.05×10^{-4}	2.03×10^{-4}
SiH_2	1.38×10^{-1}	1.30×10^{-1}	1.32×10^{-1}
SiH_3	2.60×10^{-3}	2.25×10^{-3}	2.47×10^{-3}
SiH_4	1.47×10^{-2}	1.41×10^{-2}	1.40×10^{-2}
Si_2H_2	1.20×10^{0}	1.17×10^{0}	1.15×10^{0}
Si_2H_3	1.79×10^{-5}	1.69×10^{-5}	1.77×10^{-5}
H_2SiSiH_2	5.56×10^{-1}	5.14×10^{-1}	5.20×10^{-1}
H_3SiSiH	4.50×10^{-3}	4.20×10^{-3}	4.31×10^{-3}
Si_2H_5	9.32×10^{-4}	8.65×10^{-4}	9.28×10^{-4}
Si_2H_6	1.04×10^{-3}	9.79×10^{-4}	1.12×10^{-3}
Si_3H_8	0	0	0
Si	4.52×10^{-4}	4.92×10^{-4}	4.27×10^{-4}
Si_2	1.33×10^{-2}	1.54×10^{-2}	1.22×10^{-2}
Si_3	1.50×10^{-3}	1.73×10^{-3}	1.40×10^{-3}
Total	1.92×10^{0}	1.86×10^{0}	1.96×10^{0}

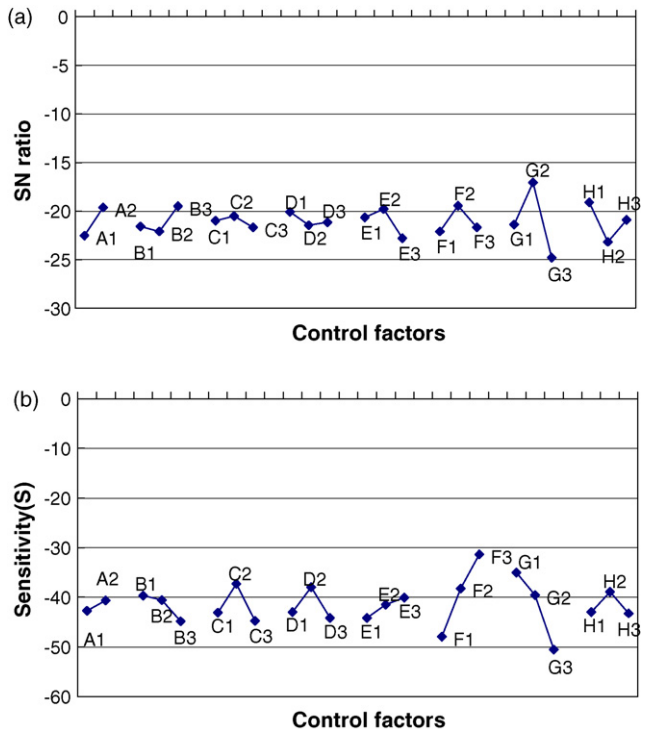

Fig. 7. The effects of (a) SN ratio and (b) the sensitivity (S) on the uniformity of deposited silicon film on the substrate in the thermal CVD process.

5. Results and discussion

5.1. Validation of computational fluid dynamics

The fluid flow, heat and mass transfer in reactor shown in Fig. 1, at $T_s = 1000$ K, $\Omega_1 = \Omega_2 = 0$, $U_{in} = 0.1$ m/s, and $T_{in} = 300$ K, are calculated for validation of CFD in the present work. The contours of velocity and temperature in the axial direction are plotted as a function of the height above the susceptor at $r = 0$ shown in Figs. 4 and 5, respectively. These figures display that the profiles of velocity and temperature are strongly non-uniform in 2-D reactor, which the maximum deviation of velocity is less than 5% comparing with the benchmark solutions [17] in the axial direction.

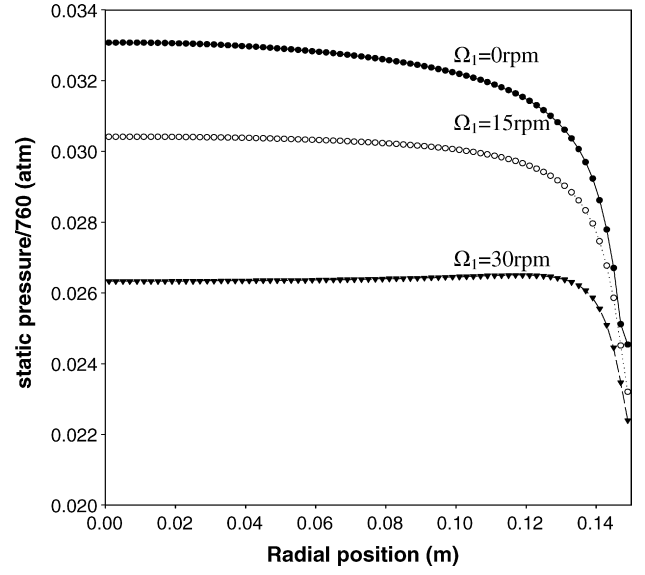

Fig. 8. The effect of rotational showerhead on pressure distribution in radius, at $\Omega_1 = 0$, 15, and 30 rpm.

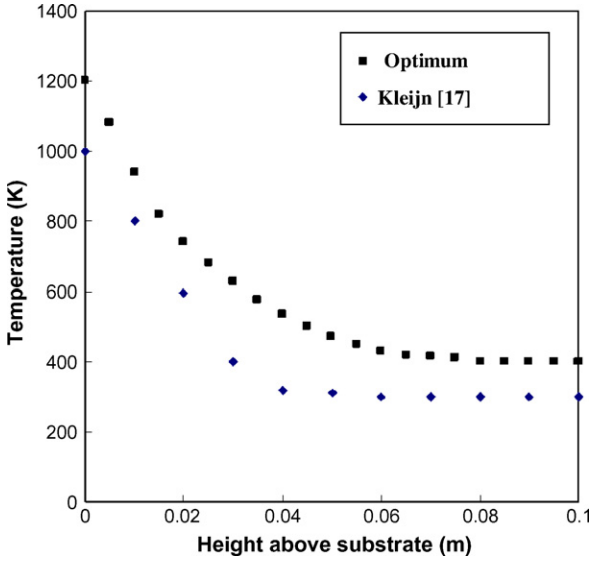

Fig. 9. Comparison of optimal conditions (circle) with process parameters presented by Kleijn [17] (solid circle) for the axial temperature profiles at $r = 0$.

In addition, applying Eq. (12), the rate of radial deposition induced by the heterogeneous decomposition of the species can be obtained with

$$\frac{dh}{dt} = \frac{R^s M_{si}}{\rho_{si}}, \tag{22}$$

where M_{si} =0.028086 (kg/mol) is the molecular weight of silicon and $\rho_{si} = 2330(kg/m^3)$ is the density of solid silicon [29]. As demonstrated in Fig. 6, the rate of deposited silicon is closed to the results predicted by Kleijn [17], which the maximum relative deviation is less than 0.8% at $r = 0.13$ m.

Furthermore, at $r = 0$, as listed in Table 6, the rates of deposition are well agreement in the 1-D results calculated by SPIN code from Coltrin and coworkers [19] and the 2-D results given by Kleijn [17], which the relative deviation of total deposition rate is about 2% and 5%, respectively.

5.2. Optimization of silicon thermal CVD process

In this work, take the operational conditions listed in Table 1 as an example for studying CFD integrated Taguchi method to optimize the thermal CVD process for the uniformity of deposited silicon film on the wafer in the different diameters. According to Eq. (15) and (16), the SN ratio and the sensitivity might be obtained by calculating the film thickness difference defined in Eq. (14). The results are presented in Table 7, where the SN ratio and sensitivity are dimensioned in the decibels (dB).

Fig. 7 shows the response plots of eight control factors of $L18$ simulation for the uniformity of deposited silicon film varying with the different sizes of subtract in a thermal CVD process. Higher SN ratio was preferred because the signal of control fac-

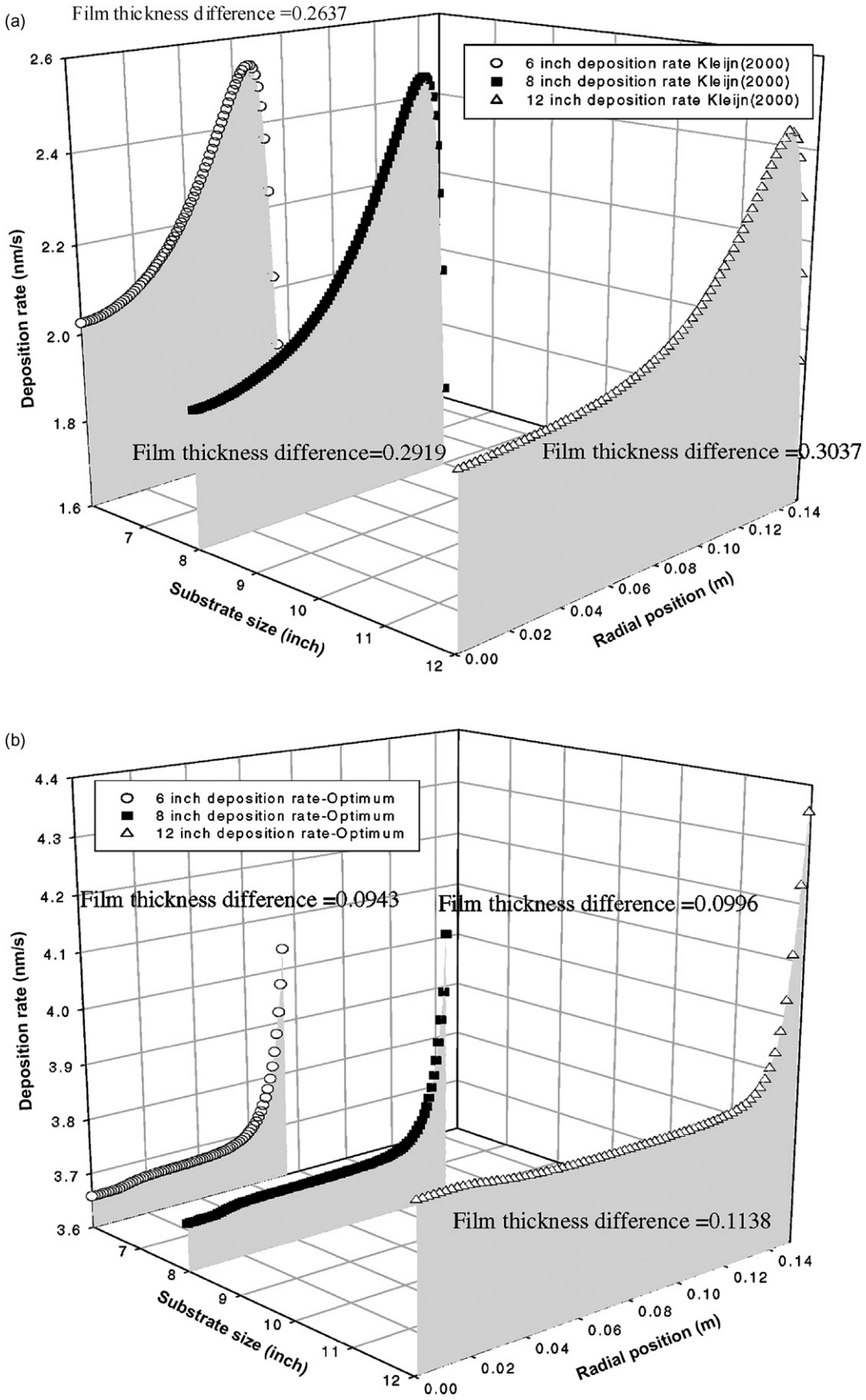

Fig. 10. The rate of deposited silicon varying with the sizes of wafer in radius for (a) the process parameters proposed by Kleijn [17] and (b) the optimal conditions, respectively.

Table 8
Effects of controlled factors and input signal on (a) SN ratio and (b) the sensitivity in the silicon thermal CVD process

Simulation no.	$M1$ ($r = 0.15$ m)	$M2$ ($r = 0.2$ m)	$M3$ ($r = 0.3$ m)	SN ratio	Sensitivity
$L1$	0.20991	0.24175	0.24296	−16.741	−40.277
$L2$	0.14494	0.12844	0.19558	−23.563	−15.346
$L3$	0.10295	0.11397	0.12614	−27.189	−48.311
$L4$	0.08812	0.06124	0.07099	−24.457	−51.005
$L5$	0.86928	0.90912	0.95693	−16.919	−28.384
$L6$	0.09941	0.12165	0.14619	−26.364	−52.286
$L7$	0.15093	0.16164	0.16694	−23.183	−45.918
$L8$	0.12002	0.13751	0.14727	−25.252	−61.337
$L9$	0.21475	0.20552	0.20502	−18.978	−41.498
$L10$	0.12904	0.14874	0.14994	−17.264	−44.656
$L11$	0.15959	0.16797	0.18839	−25.698	−46.898
$L12$	0.18286	0.20059	0.21012	−19.014	−42.401
$L13$	0.20356	0.24375	0.27569	−28.671	−47.660
$L14$	0.74734	0.85171	0.92792	−15.023	−28.866
$L15$	0.47027	0.47341	0.38562	−21.244	−35.393
$L16$	0.76851	0.83564	0.90978	−15.576	−28.982
$L17$	0.14912	0.18041	0.18654	−16.552	−42.977
$L18$	0.09135	0.09556	0.09812	−17.339	−48.084

tors is more than that of the noise [21]. Therefore, the process conditions with the maximum values of SN ratio are selected to reduce the film thickness difference of disposed silicon film on the substrate in the different sizes. As a result, the optimal conditions minimizing the thickness deviation of deposited silicon film on the substrate in the different sizes in the thermal CVD process are selected as $A_2B_1C_2D_2E_2F_3G_2H_2$ in which the subscript indicates the levels of control factor, as indicated in Table 8. These parameters can be used to obtain the gain value of 1.97 comparing with the operational conditions from Kleijn [17] in the thermal silicon CVD process, as shown in Table 9. It is found that the rotational showerhead opposing to the rotational susceptor is significantly impact on the uniformity of deposited silicon film on wafer due to uniform pressure field in radius, as illustrated in Fig. 8. In addition, at the position of $r = 0$, Fig. 9 displays that the axial temperatures of optimal conditions are higher than that of process conditions presented from Kleijn [17]. This suggests, in the thermal CVD process, raising temperature of the substrate accelerates the chemical reaction in heterogeneous phase leading to speed the migration of deposited silicon for the uniform of deposited film. Therefore, the developed optimal conditions are reasonable to increase the uniformity of deposed silicon film in thermal CVD process. As shown in Table 9, the value of β is drastically reduced from 0.01221 to 0.00387 when the obtained optimal conditions are applied in the silicon thermal CVD process.

Fig. 10 demonstrates the rate of deposited silicon varying with the sizes of wafer and the position in radius for (a) the process parameters proposed by Kleijn [17] and (b) the optimal conditions in this work. As observed in the figure, with the optimal condition, the film thickness deviation of disposed silicon on the substrate can be reduced to 9%, 10%, and 11% from 26%, 29%, and 30% for the wafer in diameters of 0.15 m, 0.2 m, and 0.3 m, respectively.

Furthermore, according to Eq. (14), the uniformity of deposited silicon film varying with the sizes of the substrate is plotted in Fig. 11 to compare the presented result with the process conditions given from Kleijn [17]. As shown in the figure, the film thickness difference of disposed silicon can be reduced to 5.8% and 11% from 18% and 36% over a wafer in diameters

Table 9
Verification of optimum conditions for the silicon thermal CVD process

Operational conditions	SN ratio	Sensitivity	β
A1B1C2D1E1F2G1H3 [17]	−20.98	−38.9	0.01221
A2B1C2D2E2F3G2H2 (present)	−19.01	−48.2	0.00387
Gain		1.97	

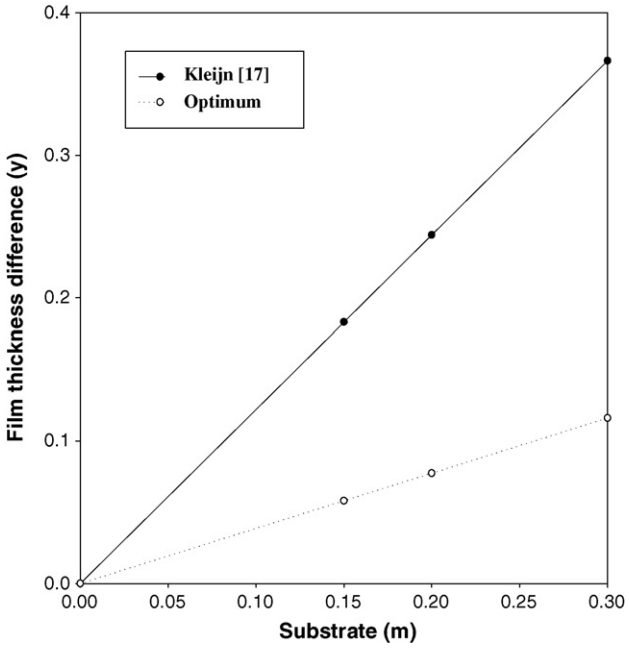

Fig. 11. The uniformity of radial deposited silicon film varying with the sizes of the substrate at the process conditions from Kleijn [17] and optimal conditions, respectively.

of 0.15 m and 0.3 m, respectively, by means of the correlation, $y = 0.00387M$.

6. Conclusion

This paper has successfully employed a commercial package of FLUENT code to simultaneously solve the two-dimensional flow, heat transfer, and multi-species chemistry in the rotating reactor with and without a rotational showerhead under steady state; and integrated the Taguchi method with a slope of dynamic model to optimize the thermal CVD process for the uniformity of silicon film varying with the different diameters of wafer. As shown in the results, through a dynamic formula, namely, $y = 0.00387M$, developed in this work, film thickness difference of deposited silicon can be reduced to 6% and 11% over the wafers in diameters of 0.15 m and 0.3 m, respectively, because the non-uniform pressure profile in radius was significantly damped in the thermal CVD process.

Hopefully, these results will generate sufficient interest so that future studies can ascertain the computational fluid dynamics integrating with Taguchi method being used to optimize other thin film process for the scale up of advanced materials and development of novel opto-electronics next revolution of information and communication in the future.

Acknowledgement

This work was partly supported by a grant NSC 89-2216-E-005-017 from the National Science Council of Republic of China.

References

[1] S.M. Sze, The Physics of Semiconductor Devices, Wiley, New York, 1981.
[2] A.C. Jones, P. O'Brien, CVD of Compound Semiconductors, VCH, Weinhein, Germany, 1997.
[3] T. Tsukada, Liquid Crystal Displays Addressed by Thin Film Transistors, Gordon and Breach Publishers, 1996.
[4] G. Wahl, The transport phenomena model of APCVD, Thin Solid Films 40 (1977) 13–26.
[5] M.E. Coltrin, R.J. Kee, J. Miller, A mathematical model of the coupled fluid mechanics and chemical kinetics in a chemical vapor deposition reactor, J. Electrochem. Soc. 131 (1984) 425–434.
[6] M. Tirtowidjojo, R.J. Pollard, The surface reaction of chemical vapor deposition, Cryst. Growth 77 (1988) 108–119.
[7] J. Ouazzani, K. Chiu, F.J. Rosenberger, On the 2D modeling of horizontal cvd reactors and its limitations, J. Cryst. Growth 91 (1988) 497–508.
[8] W.G. Breiland, M.E. Coltrin, Si deposition rates in a two-dimensional CVD reactor and comparisons with model calculations, J. Electrochem. Soc. 137 (1990) 2313–2319.
[9] C.R. Kleijn, C.J. Hoogendoorn, A study of 2- and 3-transport phenomena in horizontal chemical vapor deposition reactors, Chem. Eng. Sci. 46 (1991) 321–334.
[10] D.E. Kotecki, R.A. Conti, S.G. Barbee, T.D. Cacouris, J.D. Chapple-Sokol, R.J. Eschabach, D.L. Wilson, J. Wong, S.P. Zuhoski, Applications of computational fluid dynamics for improved performance in chemical-vapor-deposition reactors, J. Vac. Sci. Technol. B 12 (1994) 2752–2757.
[11] C. Werner, M. Ilg, K. Uram, Three-dimensional equipment modeling for chemical vapor deposition, J. Vac. Sci. Technol. A 14 (1996) 1147–1151.
[12] M.E. Coltrin, R.J. Kee, J.J. Miller, A mathematical model of silicon chemical vapor deposition, J. Electrochem. Soc. 133 (1986) 1206–1213.
[13] W.G. Breiland, M.E. Coltrin, P. Ho, Comparisons between a gas-phase model of silane chemical vapor deposition and laser-diagnostic measurements, J. Appl. Phys. 59 (1986) 3267–3273.
[14] R.J. Buss, P. Ho, W.G. Breiland, M.E. Coltrin, Reactive sticking coefficients for siliane and disilane on polycrystalline silicon, J. Appl. Phys. 63 (1988) 2808–2819.
[15] M.E. Coltrin, R.J. Kee, G.H. Evans, A mathematical model of the fluid mechanics and gas-phase chemistry in a rotating disk chemical vapor deposition reactor, J. Electrochem Soc. 136 (1989) 819–829.
[16] M.D. Allendorf, R.J. Kee, A model of silicon carbide chemical vapor deposition, J. Electrochem. Soc. 138 (1991) 841–852.
[17] C.R. Kleijn, Computational modeling of transport phenomena and detailed chemistry in chemical vapor deposition—a benchmark solution, Thin Solid Film 365 (2000) 294–306.
[18] R.J. Kee, F.M. Rupley, J.A. Miller, Chemkin-II: A FORTRAN chemical kinetics package for the analysis of gas-phase chemical kinetics, Technical Report SAND89-8009B, UC-706, SANDIA National Laboratories, Ailbuquerque, NM, 1989.
[19] M.E. Coltrin, R.J. Kee, G.H. Evans, E. Meeks, F.M. Rupley, J.F. Grcar, SPIN (version 3.83): a FORTRAN program for modeling one-dimensional rotatingdisk/stagnation-flow chemical vapor deposition reactors, Reaction Design, Inc., 11436 Sorrento Valley Road, San Diego, CA 921121, USA, Technical Report SAND93-8003, UC-401, SANDIA National Laboratories, Ailbuquerque, NM/Livermore, 1993.
[20] M.E. Coltrin, R.J. Kee, F.M. Rupley, E. Meeks, Surface Chemkin III, Reaction Design, Inc., 11436 Sorrento Valley Road, San Diego, CA 921121, USA, Technical Report SAND96-8217, UC-401, SANDIA National Laboratories, Ailbuquerque, NM/Livermore, 1996.
[21] R.A. Wysk, B.W. Niebel, P.H. Cohen, T.W. Simpson, Manufacturing Process: Integrated Product and Process Design, McGraw Hill, New York, 2000.
[22] D. Rajkumar, T. Nguty, N.N. Ekere, IEEE/CPMT International Electronic Manufacturing Technology Symposium, Santa Clara, CA, 2000.
[23] C.S. Tsai, Evaluation and optimization of integrated manufacturing system operations using Taguch's experiment design in computer simulation, Computers Industrial Engineering 43 (2002) 591–604.
[24] S.M. Wang, Y.S. Giang, Y.C. Ling, Taguchi's method in optimizing the experimental conditions of simultaneous supercritical fluid extraction and chemical derivatization for the gas chromatographic–mass spectrometric determination of amphetamine and methamphetamine in aqueous matrix, Forensic Sci. J. 1 (2002) 47–53.
[25] C.H. Chien, Y.C. Chen, Y.T. Chiou, T. Chen, C.C. Hsieh, J.J. Yan, W.Z. Chen, Y.D. Wu, Influences of the moisture absorption on PBGA package's warpage during IR reflow process, Microelectronics Reliability 43 (2003) 131–136.
[26] G.P. Syrcos, Die casting process optimization using Taguchi methods, J. Mater. Process. Technol. 135 (2003) 68–74.
[27] R.B. Bird, W.E. Stewart, E.N. Lightfoot, Transport Phenomena, Wiley, New York, 1960.
[28] C.R. Kleijn, in: M. Meyyappan (Ed.), Computational Modeling in Semiconductor Processing, Artech House, Boston, MA, 1995, p. 97.
[29] S. Wolf, Silicon Processing for the VLSI Era, vol. I, Lattice Press, 1986.